



Genotype Specific Photosynthesis x Environment Interactions Captured by Automated Fluorescence Canopy Scans Over Two Fluctuating Growing Seasons

OPEN ACCESS

Edited by:

Kelly R. Thorp,
U.S. Arid Land Agricultural Research
Center (USDA ARS),
United States

Reviewed by:

Hazem M. Kalaji,
Warsaw University of Life Sciences -
SGGW, Poland
Keshav Dahal,
Agriculture and Agri-Food Canada,
Canada
Vladimir Sukhov,
N. I. Lobachevsky State University of
Nizhny Novgorod,
Russia

*Correspondence:

Beat Keller
beat.keller@usys.ethz.ch

†Present address:

Beat Keller
Molecular Plant Breeding,
Institute of Agricultural Sciences,
ETH Zurich,
Zurich, Switzerland

Specialty section:

This article was submitted to
Technical Advances in Plant Science,
a section of the journal
Frontiers in Plant Science

Received: 28 June 2019

Accepted: 25 October 2019

Published: 20 November 2019

Citation:

Keller B, Matsubara S, Rascher U,
Pieruschka R, Steier A, Kraska T and
Muller O (2019) Genotype Specific
Photosynthesis x Environment
Interactions Captured by Automated
Fluorescence Canopy Scans Over
Two Fluctuating Growing Seasons.
Front. Plant Sci. 10:1482.
doi: 10.3389/fpls.2019.01482

Beat Keller^{1†}, Shizue Matsubara¹, Uwe Rascher¹, Roland Pieruschka¹, Angelina Steier¹,
Thorsten Kraska² and Onno Muller¹

¹ IBG-2: Plant Sciences, Institute of Bio- and Geosciences, Forschungszentrum Jülich GmbH, Jülich, Germany, ² Field Lab
Campus Klein-Altendorf, University of Bonn, Rheinbach, Germany

Photosynthesis reacts dynamic and in different time scales to changing conditions. Light and temperature acclimation balance photosynthetic processes in a complex interplay with the fluctuating environment. However, due to limitations in the measurements techniques, these acclimations are often described under steady-state conditions leading to inaccurate photosynthesis estimates in the field. Here we analyze the photosynthetic interaction with the fluctuating environment and canopy architecture over two seasons using a fully automated phenotyping system. We acquired over 700,000 chlorophyll fluorescence transients and spectral measurements under semi-field conditions in four crop species including 28 genotypes. As expected, the quantum efficiency of the photosystem II (F_v/F_m in the dark and F_q'/F_m' in the light) was determined by light intensity. It was further significantly affected by spectral indices representing canopy structure effects. In contrast, a newly established parameter, monitoring the efficiency of electron transport (F_{r2}/F_v in the dark respective F_{r2}'/F_q' in the light), was highly responsive to temperature (R^2 up to 0.75). This parameter decreased with temperature and enabled the detection of cold tolerant species and genotypes. We demonstrated the ability to capture and model the dynamic photosynthesis response to the environment over entire growth seasons. The improved linkage of photosynthetic performance to canopy structure, temperature and cold tolerance offers great potential for plant breeding and crop growth modeling.

Keywords: cold acclimation, photosynthesis x environment interactions, electron transport, chlorophyll fluorescence, high-throughput phenotyping

INTRODUCTION

Photosynthesis is a highly dynamic process responding to environmental changes, especially to light intensity and temperature, in short- and long-term acclimation (Demmig-Adams et al., 2012; Kono and Terashima, 2014). Excess light energy is dissipated within seconds upon thylakoid lumen acidification, known as non-photochemical quenching (NPQ) (Noctor et al., 1991; Adams III et al., 2006; Croce, 2015). This protection status can last or relaxes within minutes (Demmig-Adams et al., 2012; Kromdijk et al., 2016). In contrast, acclimation and deacclimation to low temperature is

slower requiring up to a few days (Huner et al., 1993; Rapacz et al., 2008; Zuther et al., 2015). Photosynthetic performance at low temperature is tightly linked to cold tolerance (Rapacz et al., 2008; Dahal et al., 2012). Traits reflecting cold tolerance in the field are an important breeding target in order to adapt crop productivity to a colder and changing climate (Rapacz et al., 2014; Frascaroli, 2018). However, photosynthetic regulation under natural fluctuating conditions, especially in response to temperature, is hardly known (Rogers et al., 2017; Murchie et al., 2018).

Cold acclimation is initiated, amongst other factors, by an imbalance between photosynthetic energy uptake and the metabolomic sink (Huner et al., 1998; Ensminger et al., 2006; Hüner et al., 2012). At low temperatures, cold responsive genes trigger different acclimation processes regulating, e.g., the expression of hormones, chloroplast proteins, and proteins associated with lipid metabolism (Svensson et al., 2006; Liu et al., 2019). Differences in cold tolerant and sensitive barley genotypes were reported in expression of cold responsive genes and photosynthetic capacity at low temperature (Rapacz et al., 2008). Photosynthesis itself acclimates to cold temperature by synthesizing more photosynthetic proteins since enzyme activity is decreased and by maintaining greater membrane fluidity (Yamori et al., 2014). Membrane fluidity at high and chilling temperatures is adjusted by the amount of trienoic fatty acids in the chloroplast and thylakoid membrane (Mitchell and Barber, 1986; Murakami et al., 2000; Sage and Kubien, 2007). This process ensures the optimal function of proteins integrated into the membrane and diffusion of electron carriers for photosynthetic electron transport (Upchurch, 2008; Liu et al., 2013). In consequence, temperature acclimation and chilling stress alter electron transport kinetics between photosystem II (PSII) and photosystem I (PSI) (Yamasaki et al., 2002; Suzuki et al., 2011).

Photosynthesis under field conditions is complex not only because of the fluctuating environment but also due to the canopy structure. Sunlight flecks which occur by canopy movement and light penetration into the canopy alter the photosynthetic status (Jia et al., 2013; Kono and Terashima, 2014; Townsend et al., 2018; Kaiser et al., 2018b). Consequently, photosynthetic light responses differ in controlled versus field conditions (Rascher and Nedbal, 2006; Meacham et al., 2017; Vialet-Chabrand et al., 2017). Leaves grown under fluctuating conditions showed lower photosynthetic capacity compared to controlled conditions but similar photosynthetic rates per leaf area (Vialet-Chabrand et al., 2017). In addition, leaves in the lower canopy acclimate to shading with decreasing photosynthesis and nitrogen content (Evans and Poorter, 2001; D'Odorico et al., 2019). Sunlight flecks interfere with this acclimation process and high net photosynthetic rates are maintained (Kaiser et al., 2018a).

In order to understand the dynamic regulation and acclimation of canopy photosynthesis in response to a fluctuating environment, high-throughput photosynthesis phenotyping systems are required with a high spatio-temporal resolution. Chlorophyll fluorescence (ChlF)-based measurements serve as a fast proxy for net photosynthesis derived from CO₂ gas exchange measurements (Warren and Dreyer, 2006; Fiorani and Schurr, 2013; Kalaji et al., 2017). However, existing ChlF phenotyping

platforms operate under static conditions and are not able to catch natural environmental interactions (Jansen et al., 2009; Mishra et al., 2014; Flood et al., 2016; Wang et al., 2018). Under field conditions, measurements are usually carried out manually and restricted to a few days and to the leaf level (Rapacz et al., 2004; Ribeiro et al., 2004; Demmig-Adams et al., 2012; Moura dos Santos et al., 2013). ChlF-based operating efficiency of PSII (F_q'/F_m') is widely used to assess photosynthetic performance (Baker, 2008; Kalaji et al., 2016). F_q'/F_m' is sensitive to light, as it is affected by the amount of NPQ at the PSII antennae (Von Caemmerer, 2000; Croce, 2015; Lázár, 2015). However, changes in electron transport between PSII and PSI, which occur in response to temperature, are difficult to detect using F_q'/F_m' because it represents the efficiency of charge separation in the PSII reaction center (Van Heerden et al., 2003; Bezouw et al., 2019).

The light-induced fluorescence transient (LIFT) method monitors ChlF induction and relaxation within milliseconds from a distance using sub-saturating excitation flashlets (Kolber et al., 1998; Pieruschka et al., 2010; Osmond et al., 2017; Keller et al., 2019). The efficiency of PSII charge separation (F_q'/F_m') is derived from ChlF induction using fast repetition rate flashlets (Kolber et al., 1998). Electron transport rates derived by the LIFT method from several meter distance were highly correlated to pulse amplitude modulated and gas exchange measurements from close distance (Pieruschka et al., 2010). Further, the efficiency of electron transport beyond the primary quinone electron acceptor of PSII (Q_A) in the dark (F_r/F_v) and light (F_r'/F_q') can be assessed *via* ChlF relaxation using flashlets with decreasing repetition rate. F_r/F_v serves as a fast and robust approximation of electron transport kinetics (Keller et al., 2019). From a series of saturating flashes in the dark and the followed ChlF relaxation, it was observed that Q_A^- oxidation time constants are approximately 0.2 ms to reduce the secondary quinone electron acceptor (Q_B) and 0.7 ms to reduce Q_B^- to Q_B^{2-} (Vass et al., 1999; de Wijn and van Gorkom, 2001). The time constant of binding a plastoquinone (PQ) to a vacant Q_B -binding site is about 2 to 3 ms which matches roughly the estimated turn-over time for a oxidized PQ to leave the Q_B pocket side as reduced plastoquinol (PQH₂) (de Wijn and van Gorkom, 2001; Petrouleas and Crofts, 2005). In the light, the ChlF relaxation showed less pronounced phases and F_r'/F_q' derived thereof was rather insensitive to increasing light intensities (Keller et al., 2019). Besides, the LIFT device acquires the leaf reflectance spectrum. Spectral indices such as the photochemical reflectance index (PRI) are correlated to photosynthetic light use efficiency, chlorophyll content, and related to canopy structure (Barton and North, 2001; Shrestha et al., 2012; Wu et al., 2015; Schickling et al., 2016; Sukhova and Sukhov, 2018).

We established a fully automated LIFT high-throughput phenotyping system and monitored four crop species (barley, maize, soybean, wheat) over two growing seasons. The main hypothesis was that F_r'/F_q' is independent of F_q'/F_m' bearing additional information to photosynthetic activity and its regulation under controlled and fluctuating conditions. Specifically the following hypotheses were addressed: 1) light intensity controls the PSII efficiency of charge separation (F_q'/F_m'). The light penetration into the canopy can be approximated by reflectance indices. In contrast, 2) F_r/F_v and F_r'/F_q' show a strong dependency on temperature

which is extenuated in winter hard species and cold tolerant genotypes. F_v/F_m and F_v'/F_q' quantifies electron transport capacity indicating genotypic specific cold acclimation. 3) Fluctuating photosynthetic response and genotype x environment interactions can be modeled to predict photosynthetic performance for entire and future growing seasons.

For the first time, we quantified F_v/F_m under controlled and fluctuating conditions. In addition, full reflectance spectra of the measured leaves were acquired to gain information about canopy structure. We show the photosynthetic response over the full growing season beyond snapshot phenotyping toward the full incorporation of genotype x environmental interactions using high-throughput data and modeling. F_v/F_m proved to be a promising trait to study photosynthetic regulation and cold tolerance.

MATERIAL AND METHODS

ChlF measurements were performed under controlled and semi-field conditions in five species and 29 genotypes by using the LIFT method in high-throughput.

Controlled Conditions

Arabidopsis (*Arabidopsis thaliana*) Col-0 genotypes were grown at 23°C in 12/12 h day/night cycle in the growth chamber at around 150 $\mu\text{mol photons m}^{-2} \text{s}^{-1}$. At 59 days after sowing (DAS), plants were subjected for four days to fluctuating temperature between 15 and 35°C. The temperature increased in the light and decreased in the dark. Temperature steps were 5°C in 2 h intervals followed by 4 h at 20°C. The air humidity in the climate chamber was kept at around 50–70%.

Semi-Field Growth Conditions

The *Miniplot* facility with an automated measuring platform is located at the Field Campus Klein Altendorf (University of Bonn, Germany, 50°37' N, 6°59' E) in an unheated glasshouse without additional lighting (Thomas et al., 2018). The *Miniplot* facility hosts a total of 90 growth containers (111 x 71 x 61 cm) with a volume of 535 L filled with a loamy-clay silt soil (luvisol) from the nearby field site (Hecht et al., 2016). Containers were drip irrigated with approximately 16 L per week. The amount was increased to up to 36 L per week in hot weather conditions.

Soybean

Soybean [*Glycine max* (L.) Merr.] genotypes differing in cold tolerance were kindly provided by the Swiss soybean breeding program of Agroscope (Changins, Switzerland). Genotypes Amarok, Gallec, and Tourmaline are tolerant to cold whereas 22216, S1, and Protibus are cold sensitive (Supplementary Table 1) (Gass et al., 1996). In 2016, soybean genotypes were sown on August 19 directly into the containers of the *Miniplot* facility. 22 seeds per container were sown 3 cm deep in two rows (distance 40 cm) every 10 cm. Five genotypes in two replicates and one genotype (S1) in 1 replicate were planted in 11 randomized containers. On September 20, each container was fertilized with 30 g Hakaphos® Blue (N-P-K, 1.0–0.7–1.0, COMPO EXPERT GmbH, Münster, Germany).

In 2017, Genotype Protibus was excluded Bahia, Eiko, and MinnGold were included into the trial. The MinnGold genotype has a chlorophyll-deficient phenotype caused by a spontaneous mutation in the Mg-chelatase subunit gene (*ChlI1a*) (Campbell et al., 2015). These eight soybean genotypes were cultivated in a greenhouse for two weeks at approximately 20°C. Then on March 23, plants were transplanted into containers in the *Miniplot*. Sixteen plants per container were arrayed into two rows (40 cm row distance). Six genotypes in four replicates and two genotypes (Bahia and Eiko) in two replicates were planted in 28 containers in a randomized block design. At 34 DAS, plants were fertilized using 24 g Hakaphos® blue (COMPO EXPERT GmbH) per plot (around 3.6 g N per plot or 0.2 g N per plant). The LIFT instrument beam was focused at 1.4 m until June 21, 2017 and then adjusted to 1.2 m.

Maize

Five maize (*Zea mays*) genotypes of the German Plant Phenotyping Network (DPPN) reference collection were sown on May 24, 2016 (Supplementary Table 2). Genotypes were grown in 10 containers in a randomized block design (two containers per genotype). In 2017, nine genotypes of the DPPN reference were sown on May 30 into 18 containers.

Barley

Six commercial available barley (*Hordeum vulgare* L.) cultivars (Gesine, Eileen, Irina, Tocada, Grace, and Milford) were selected (Bundessortenamt, 2013). These cultivars were sown on September 16, 2016 in one container per genotype and grown as described in Thomas et al. (2018). The sowing density per plot was 360 seeds.

Wheat

Three wheat (*Triticum aestivum* L.) genotypes (Brilhante, PF37 and PF62) were used in this study (Poersch-Bortolon et al., 2016). Fifty seeds per meter in 15 cm row distance (five rows per container) were sown on May 12, 2016 into six containers (two containers per genotype) in a randomized block design. On June 15, 30 g Hakaphos® Blue (COMPO EXPERT GmbH) per container was applied.

Environmental Data

Environmental data were recorded every minute from three sensor stations distributed in the *Miniplot* facility. Data were uploaded to an SQL database. The used sensors were LI-190 (LI-COR Inc., Nebraska USA) for photosynthetic photon flux density (PPFD) and HMP110 (Vaisala, Helsinki, Finland) for air temperature and humidity. Environmental data were linked to LIFT measurements taken in the same minute.

Light-Induced Fluorescence Transient Device

The compact LIFT instrument (Version LIFT-REM, Soliense Inc., New York, USA) is equipped with a blue light-emitting diode (LED) (445 nm), a STS-VIS spectrometer (Ocean Optics, Florida, USA), and two RGB cameras (FLIR Integrated Imaging

Solutions Inc., British Columbia, Canada). Subsaturating actinic LED flashlets in fast repetition rate (FRR) induce the maximum fluorescence yield and monitor its relaxation with decreasing repetition rates. ChlF is detected at 685 (± 10) nm. The FRR flash was used with an excitation phase of 0.75 ms ($\text{FRRF}_{0.75\text{ms}}$) consisting of 300 flashlets (Keller et al., 2019). The relaxation phase included 127 flashlets triggered at decreasing repetition rate and lasted for 200 ms (**Figure 1A**). When measuring under ambient light, background irradiation in the wavelength range of the detector is determined between the flashlets and subtracted from the ChlF yield of every flashlet. For all measurements, the excitation power at 60 cm distance was about 40,000 photons $\text{m}^{-2} \text{s}^{-1}$ for the ChlF induction phase, as described in Keller et al. (2019).

Light Response Curves Under Controlled Conditions

Blue light curves at different temperatures were carried out on *Arabidopsis* plants. Plants were dark adapted for 30 min prior to measurements ($n = 5$ plants). The light response curve consisted

of 161 $\text{FRRF}_{0.75\text{ms}}$. It was one $\text{FRRF}_{0.75\text{ms}}$ in the dark-adapted state and 40 $\text{FRRF}_{0.75\text{ms}}$ at each light intensity level in a 1.5 s interval. Light intensities were 80, 100, 200, 400 $\mu\text{mol photons m}^{-2} \text{s}^{-1}$. Plants were measured from low to high light intensities at 25°C, 35°C (63 DAS), and the following day at 20, 15, and 30°C (64 DAS). Transition between temperatures took about 20 min. LI-COR sensors were matched at every temperature step and after every second measurement.

The blue LED of the LIFT instrument was used as actinic light source (445 nm). The size of the illumination spot was around 3 cm^2 . The intensity of the blue LED was calibrated by using a quantum sensor (LI-190R, LI-COR, Inc.) at 60 cm distance. A fully expanded leaf was placed into a LI-6400XT transparent 2x3 cm chamber head (LI-COR, Inc., Nebraska USA) and measured with the LIFT instrument through the transparent film of the chamber. The air flow rate during the measurements was 300 $\mu\text{mol air s}^{-1}$ and block temperature was kept at 20°C. CO_2 concentration in the air was controlled at 400 ppm and air flow was set to 400 $\mu\text{mol s}^{-1}$.

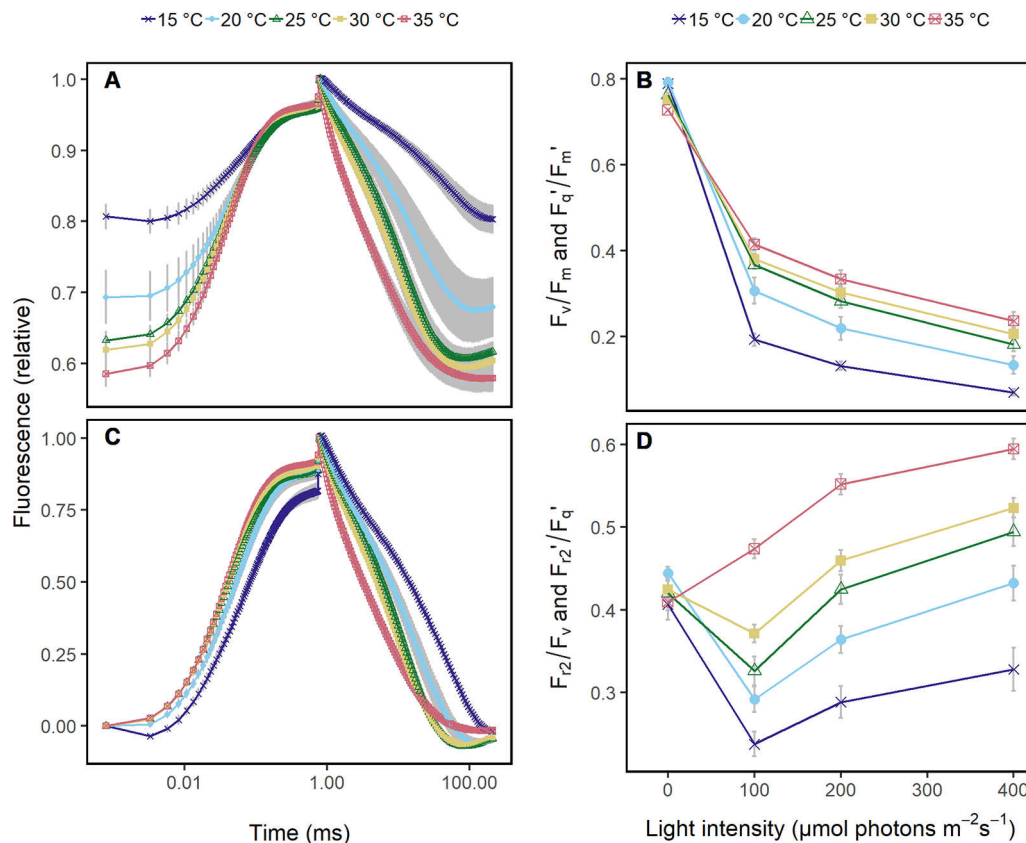


FIGURE 1 | Chlorophyll fluorescence transients were acquired in *Arabidopsis* leaves from 60 cm distance using fast repetition rate excitation flashlets. Leaves were subjected to different temperatures (15 to 35°C) and different light intensities under controlled laboratory conditions. **(A)** Transient was normalized to the maximum chlorophyll fluorescence which allows to compare the quantum efficiency of the photosystem II (F_v/F_m in the dark and F_q'/F_m' in the light) at the different temperatures. The ambient light intensity was 200 $\mu\text{mol photons m}^{-2} \text{s}^{-1}$. **(B)** F_v/F_m and F_q'/F_m' in response to increasing light intensities at the different temperatures are shown. **(C)** Chlorophyll fluorescence transients in (A) were double normalized to the maximum and minimum chlorophyll fluorescence, which allows to retrieve the efficiency of electron transport 5 ms after reduction of the primary quinone (Q_A) (F_2/F_v in the dark, F_2'/F_q' in the light). **(D)** F_2/F_v and F_2'/F_q' are shown in response to increasing light intensities at the different temperatures. Attached *Arabidopsis* leaves ($n = 6$) were measured in dark-adapted and steady-state at 0, 100, 200, and 400 $\mu\text{mol photons m}^{-2} \text{s}^{-1}$ of blue light (445 nm). Error bars indicate the 95% confident interval.

Automated Measurements Under Fluctuating Semi-Field Conditions

Fully automated LIFT measurements took place from May 2016 to August 2017 using the measuring platform of the *Miniplot* facility (**Figure 2A**). Every hour, crop canopy of every container was scanned in consecutive 3 x 300 mm line measurements at a velocity of around 30 mm s⁻¹ by one or two LIFT devices. The distance from the LIFT lens to soil was 1.5 m and the measurements were initially focused at 1.4 m. The focus was adjusted as plants grew. The measuring spot was around 30 mm in diameter, hence about 700 mm² (**Figure 2B**). Each ChlF transient measurement took 210 ms. Every ChlF measurement was followed by a spectral measurement with 1,790 ms integration time (**Supplementary Figure 1A**). In that mode, one combined measurement was acquired every 2 s, resulting in 5 to 7 combined measurements for each of the 3 x 300 mm scans (**Supplementary Figure 2**). In total, about 18 independent measurements were acquired for each row operating with one LIFT device. The third measurement of each line was excluded since it most likely measured the same spot due to the stop of the positioning system after 300 mm. For the experiments in 2017, it was about 36 measurements since two LIFT devices operated simultaneously hanging next to each other from the moving platform.

Leaf Angle and Canopy Effects

In order to assess the canopy effect and different measuring distances, leaves of soybean genotype *Tourmaline* were fixed 30 cm aboveground with three needles on top of a bamboo stick perpendicular to the LIFT lens. Four leaves per plot in four plots were fixed (n = 16). Automated platform measured changing the distance randomized from 120 to 75 cm in 15 cm steps. Every leaf was measured with randomized distance in 14-min intervals allowing oxygen evolving complex to relax when measuring during the night.

Fluorescence Data Processing

The ChlF transient data acquired by the LIFT FRRF_{0.75ms} represent complex processes of Q_A reduction and reoxidation. In order to quantitatively characterize the main processes, the

ChlF transients were analyzed on an empirical basis described in Keller et al. (2019).

Retrieval of Minimum and Maximum Fluorescence

For the FRRF_{0.75ms} used in this study, the minimum ChlF yield F₀ is defined as the ChlF yield of the first flashlet and the maximum ChlF yield (F_m) as the averaged ChlF yield of the 301st and 302nd flashlet (Keller et al., 2019). The 300th flashlet does not represent F_m due to quenching processes in the induction phase. The variable ChlF yield (F_v) is the difference between F_m and F₀ which was used to calculate the maximum efficiency of PSII (F_v/F_m) in the dark-adapted state. The light adapted states of F_v and F_m were denoted as F_q' and F_m'.

Q_A- Reoxidation Efficiency

The ChlF parameter F_r/F_v represents the efficiency of reoxidation after Q_A reduction, which can be estimated by measuring the kinetics of ChlF relaxation. For calculation of F_r/F_v, the area between F_m and actual ChlF (F_{r1} or F_{r2}) was integrated within a specific time range (t₁ to t₂) during ChlF relaxation measurements and normalized to the integral area of F_v in that time range (Keller, 2018). The same calculation were made using data from light-adapted measurements. Two time ranges, t₁ to t₂, were chosen to catch reoxidation processes with different time constants:

1. t₁ from 0.8 to 1.47 ms (0.65 ms for calculation of F_{r1})
2. t₂ from 0.8 to 5.9 ms (5 ms for calculation of F_{r2})

resulting in the efficiency of electron transport 0.65 ms after reduction of Q_A (F_{r1}/F_v in the dark; F_{r1}'/F_q' in the light) and 5 ms after reduction of Q_A (F_{r2}/F_v in the dark; F_{r2}'/F_q' in the light). In contrast to the earlier study of Keller et al. (2019), the time range for t₂ was chosen to get a more detailed insight into the dynamics of ChlF relaxation. The time ranges of t₁ and t₂ correspond to the first and second exponential decay phases after ChlF induction (Vass et al., 1999). These phases are pronounced in dark-adapted samples, in which the photosynthetic apparatus is not activated, but are not visible in light-adapted samples (Keller et al., 2019).

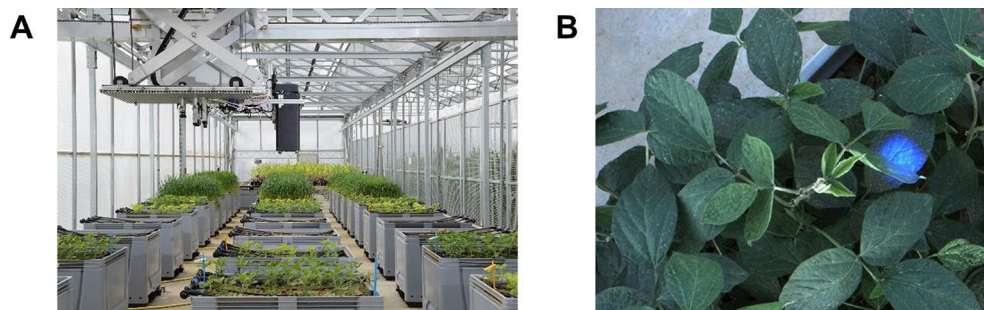


FIGURE 2 | The fully automated light-induced fluorescence transient (LIFT) system scanned crop canopy in 30 mm s⁻¹ measuring every 2 s. **(A)** Plants were grown in containers under fluctuating conditions in an unheated glasshouse. The measuring distance was about 1 m. **(B)** The diameter of the measuring beam on the canopy was around 30 mm.

Spectral Data Processing

Spectral measurements were taken from 400 to 800 nm in 0.46 nm resolution. The detector temperature of the spectrometer was kept between 20 and 35°C. Measurements were acquired in the glasshouse under ambient sunlight every 2 s during the canopy scans. Raw digital numbers from the spectrometer output were averaged to intervals of 2 nm, i.e., to one value per every full even wavelength number between 400 and 800 nm. From every spectra taken during the day, the instrument noise (dark current) measured from spectra at the night before was subtracted. The averaged wavelengths were then used to calculate pseudo spectral indices from the raw digital numbers. The pseudo spectral indices are marked with a "p" at the beginning of the abbreviation, e.g., pseudonormalized difference vegetation index (pNDVI). In addition, reflectance spectra were normalized for incoming irradiance by gray reference spectra (reflecting 50% of the total incoming irradiation). Measurements on the gray reference were carried out in the middle of every measuring round, i.e. once per hour between May 15 and May 18, 2017. The reflectance spectra were then associated with the PPFD value recorded from the environmental station in the same minute and averaged in steps of 10 $\mu\text{mol photons m}^{-2} \text{ s}^{-1}$. In that way, a look up table for reference spectra was generated for spectra covering a range from 100 to 1,350 $\mu\text{mol photons m}^{-2} \text{ s}^{-1}$. This look up table was used to correct every spectral measurement according to its associated top of canopy PPFD value using the corresponding reference spectra closest to that PPFD value [Keller (2018) and **Supplementary Figure 1**]. Normalized difference vegetation index (NDVI), alternative NDVI (NDVI_{II}), green normalized difference vegetation index (GNDVI), MERIS Terrestrial Chlorophyll Index (MTCI), and the PRI were calculated as the following:

1. NDVI = (R750–R706)/(R750+R706) adapted from Frampton et al. (2013)
2. NDVI_{II} = (R740–R680)/(R740+R680) adapted from Frampton et al. (2013)
3. GNDVI = (R740–R540)/(R740+R540) adapted from Frampton et al. (2013)
4. MTCI = (R754–R710)/(R710+R680) adapted from Dash and Curran (2004)
5. PRI = (R530–R570)/(R530+R570) adapted from Gamon et al. (1992)

with R indicating the used wavelength from the corrected signal. The same wavelengths were used to calculate the pseudo indices using the raw digital signal. A parameter called reflectance was calculated as the sum of the raw signals in all wavelengths between 450 and 800 nm. Every calculated spectral index was then associated to the ChlF measurement taken instantly before.

Statistical Analysis

Data of ChlF transients were discarded when the signal-to-noise ratio was lower than 50 in the case of maize, rapeseed, and soybean or lower than 100 in barley and wheat. Data were also excluded when F_v/F_m , (respective F_q'/F_m') or F_{r1}/F_v (respective F_{r1}'/F_q')

were lower than zero or F_{r1}/F_v and F_{r2}/F_v (respective F_{r1}'/F_q' and F_{r2}'/F_q') were higher than 0.35 and 0.8, respectively.

Values from spectral indices were removed when PPFD at that time was <30 $\mu\text{mol photons m}^{-2} \text{ s}^{-1}$ due to low S/N ratio at low light intensities. Outliers or measurement errors of spectral indices, for example when soil was targeted, were removed when the value was >1.5 times and <1.5 times the second and third quantile of all data collected per species, respectively.

Predictive Modeling

Least absolute shrinkage and selection operator (Lasso) regression was performed to identify dependent parameters on phenotypes under fluctuating conditions using *glmnet* package of R program (Friedman et al., 2010). Basic random model equation is:

$$y = \mu + Zu + \varepsilon,$$

where y is a vector of n phenotypic values, μ is a common intercept, Z is a $n \times p$ covariate matrix of p environmental and reflectance parameters, u is the random effect for every parameter, and ε is a vector of n residual. The random effects u are penalized by the ℓ^1 norm and scaled by a λ value determined by internal cross validation. Parameters for p were PPFD, temperature, humidity, vapor pressure deficit (VPD), reflectance, reflectance at 685 nm, GNDVI, NDVI, NDVI_{II}, PRI, MTCI, age of plants in DAS, measuring week and month, daytime, crop species, and genotype. The predictive models for F_v/F_m (respective F_q'/F_m') and F_{r2}/F_v (respective F_{r2}'/F_q') contained all parameters p . Models were fitted on soybean trainings datasets with standardized parameters. Trainings dataset contained either half of all the days measured, the growing season 2016 or 2017. Model predictions were validated on the remaining soybean data. Model accuracy was calculated as Pearson correlation coefficient between predicted and measured values.

Linear Modeling

Best predictive parameters for F_v/F_m (respective F_q'/F_m') and F_{r2}/F_v (respective F_{r2}'/F_q') were selected out of the Lasso model for linear modeling in order to quantify the effect of these parameters on photosynthesis. The error term was not further structured (e.g., for correlated errors) since no confidence intervals were calculated. The sum of squares was used to estimate the explained variance of each parameter. To analyze the leaf angle and canopy effect, the factors treatment (fixed vs. natural leaf angle) and distance were included in the linear model.

RESULTS

In order to understand the dynamics of photosynthesis, ChlF response was monitored from the distance under controlled and fluctuating conditions. The photosynthetic response in controlled steady-state conditions was investigated in *Arabidopsis* leaves under different light intensities and temperature levels. Under fluctuating semi-field conditions, four crop species including 28 genotypes were monitored over two growing seasons in order to analyze photosynthetic interactions with the environment.

In total, 789,475 measurements were acquired over 138 days using the automated LIFT system.

Chlorophyll Fluorescence Transients Under Controlled Conditions

Under controlled conditions, ChlF transients of *Arabidopsis* leaves at different temperatures showed differences in the induction phase (Figure 1A). As expected, F_q'/F_m' responded clearly to increasing light intensities and less pronounced to the different temperatures (Figure 1B). In contrast, ChlF relaxation phase and F_{r2}'/F_q' responded highly sensitive to temperatures (Figure 1C) but not to light intensities (Figure 1D).

F_v/F_m and F_q'/F_m' Under Fluctuating Conditions

Photosynthetic response under semi-field conditions was monitored in four crop species on canopy level (Figure 2). Barley and wheat canopy photosynthesis was monitored for one growing season, maize and soybean for two growing seasons covering a wide range of environmental fluctuations. F_v/F_m (in the dark) and F_q'/F_m' (in the light) responded highly dynamically to the fluctuating environmental conditions over the two growing seasons (Figure 3A). In a subset of a five diurnal soybean measurements, F_v/F_m and F_q'/F_m' showed a clear diurnal pattern following changes in PPFD. F_q'/F_m' values were further grouped according to PRI ranges, which are probably related to canopy structure (Figure 3B). In a linear model, PPFD explained in total 15.7% of all variance in F_q'/F_m' (including 3.7% from a square root term) (Supplementary Table 3). PRI explained 21.1%. Further, predicting variables pNDVI_II, measurement date, and pNDVI showed only a minor effect explaining 5.9, 4.3, and 4% of all variance in F_q'/F_m' , respectively. Temperature (accounting only for 0.3% of the variance), humidity, crop species, and genotype had no major effect on F_q'/F_m' . The interaction of PRI with F_q'/F_m' was rather stable and independent of PPFD (Figure 3C). The unexplained variance was 39.5%. In summary, F_v/F_m and F_q'/F_m' under fluctuating conditions were mainly dependent on PPFD and reflectance indices but little affected by temperature or measurement date.

F_r/F_v and F_{r2}'/F_q' Under Fluctuating Conditions

F_r/F_v (in the dark) and F_r'/F_q' (in the light) describe the oxidation kinetics of Q_A^- . In order to catch different steps in the electron transport, two time constants ($t_1 = 0.65$ ms and $t_2 = 5$ ms) were considered in this study. F_{r1}/F_v and F_{r1}'/F_q' were highly correlated to F_{r2}/F_v and F_{r2}'/F_q' in all four crops whereas the ratio depended on the measurement time (Supplementary Figure 3). Therefore in the following, this study is focused only on F_{r2}/F_v and F_{r2}'/F_q' . The parameter responded highly dynamically to the fluctuating environment (Figure 4A). In a data subset, F_{r2}/F_v and F_{r2}'/F_q' of barley and soybean showed a clear distinct diurnal pattern dependent on temperature and species (Figure 4B). In a linear model for F_{r2}/F_v and F_{r2}'/F_q' , temperature alone explained over 67% of all variance in F_{r2}/F_v and F_{r2}'/F_q' (Table 1). The different

months of the season and crop species accounted for 5.1 and 5% of the variance, respectively. Interestingly, winter barley had higher F_{r2}/F_v and F_{r2}'/F_q' values than soybean in cold temperature but lower values in warm temperature (Figure 4C). In contrast to F_q'/F_m' , PRI and pNDVI did not contribute significantly to variation in the data. The unexplained variance was 21%. The two monitored ChlF parameters, F_v/F_m (respective F_q'/F_m') and F_{r2}/F_v (respective F_{r2}'/F_q'), were independent from each other and changed their relation according to the time of the day (Supplementary Figure 4). In contrast to F_v/F_m and F_q'/F_m' , the parameters F_{r2}/F_v and F_{r2}'/F_q' were highly dependent on temperature.

Detection of Cold Tolerance in Soybean Genotypes

Since F_{r2}/F_v and F_{r2}'/F_q' may be a proxy for temperature dependent limitations in electron transport, it was tested whether these ChlF parameters detect cold tolerance. The response of F_{r2}/F_v and F_{r2}'/F_q' to temperature differed between the genotypes especially at low and high temperature (Figure 5A). Genotype Protibus had no data around 30°C because it was measured only in 2016. Data acquired at 5°C revealed faster ChlF relaxation in cold-tolerant genotype Amarok and Gallec compared to 22216 or S1 (Figure 5B). At 5°C, F_{r2}/F_v and F_{r2}'/F_q' between these four genotypes differed significantly whereas F_v/F_m showed no difference (Supplementary Figure 5). In contrast, these genotypes showed no clear difference in the ChlF relaxation at 20°C (Figure 5C). In summary, F_{r2}/F_v and F_{r2}'/F_q' allowed to monitor temperature tolerance of the photosynthesis in different genotypes.

Genotype x Environment Interaction and Modeling in Soybean Genotypes

The genotype specific response of the photosynthetic parameters to natural fluctuation under semi-field conditions was modeled in order to estimate genotype x environment interactions over full seasons. F_v/F_m and F_q'/F_m' as well as F_{r2}/F_v and F_{r2}'/F_q' were modeled based on environmental data and reflectance indices. Photosynthetic performance of 69 days were predicted in high time resolution using the remaining 69 days to train the model (in total 580,547 measurements). In a subset of three dates, the model based estimates of the photosynthetic parameters are shown together with the measured values as validation (Figure 6A). The prediction accuracies, expressed as the Pearson correlation coefficient of estimated and measured values, ranged between 0.7 and 0.92 for the different genotypes in F_q'/F_m' (and F_v/F_m) and F_{r2}'/F_q' (and F_{r2}/F_v), respectively (Figure 6B). The model coefficients are shown in Supplementary Table 4 and Supplementary Datasheet 2 respectively. Furthermore, we modeled genotype x environment interactions over an entire season based on the other measured season. These prediction accuracies ranged between 0.44 and 0.84 for the different genotypes in F_q'/F_m' (and F_v/F_m) and F_{r2}'/F_q' (and F_{r2}/F_v), respectively (Supplementary Figure 6). In summary, the modeling of genotype x environment interactions allowed the estimation of the photosynthetic performance also at days or entire seasons which had no measurements available.

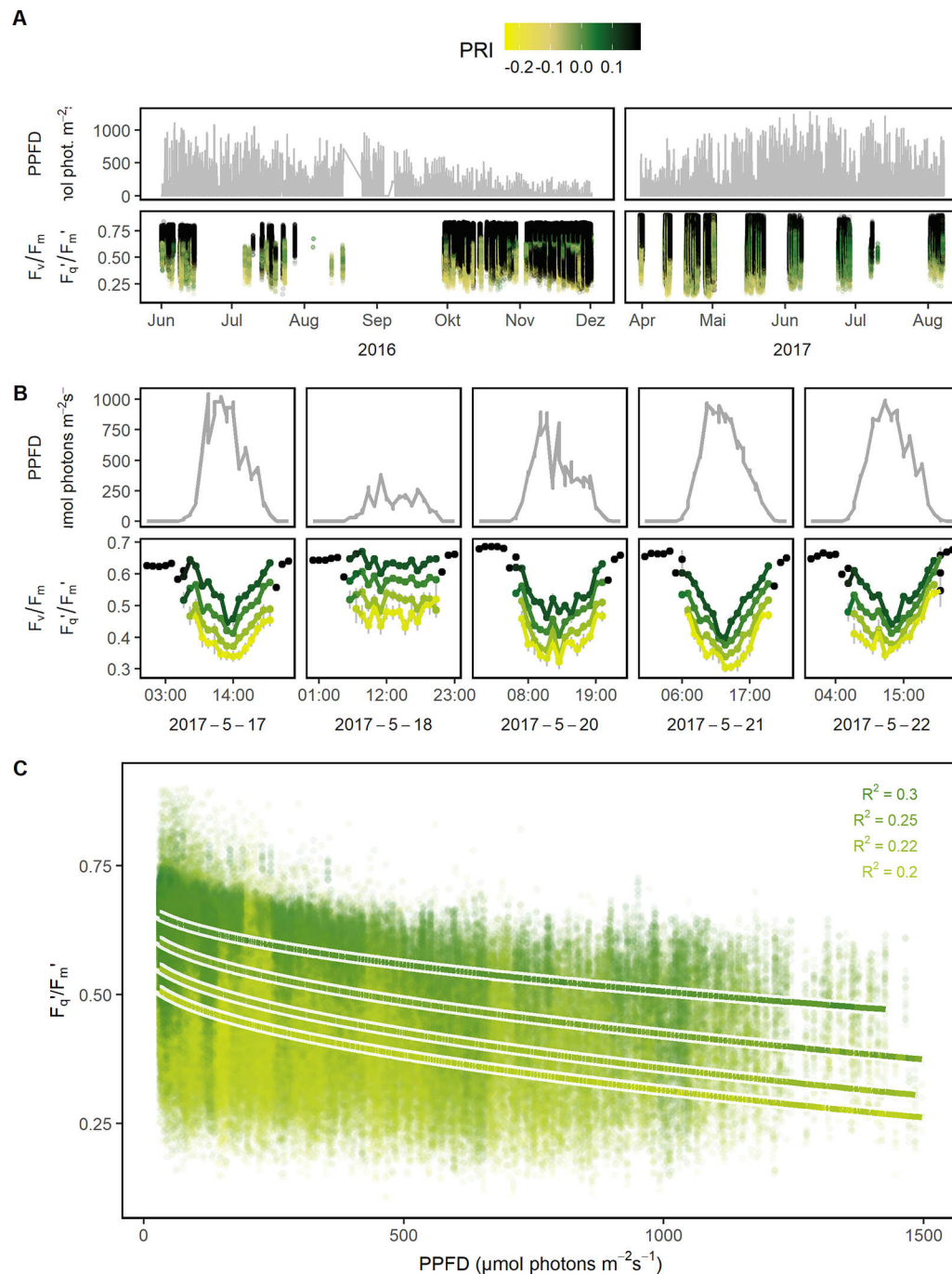


FIGURE 3 | Quantum efficiency of the photosystem II (F_v/F_m in the dark and F_q'/F_m' in the light) of barley, maize, soybean, and wheat genotypes was monitored under a fluctuating environment over two seasons in high time resolution. **(A)** Natural fluctuation of photosynthetic photon flux density (PPFD) together with the dynamic F_v/F_m and F_q'/F_m' and their associated photochemical reflectance index (PRI) values are shown over the two growing seasons ($n = 782,420$, acquired from May 2016 to August 2017). **(B)** PPFD and F_v/F_m (respective F_q'/F_m') are shown in a subset of diurnal measurements within 1 week to illustrate the strong interaction between the parameters. F_v/F_m and F_q'/F_m' were grouped according to photochemical reflectance index (PRI) levels to reveal the strong effect of PRI. Gray error bars show 95% confidence interval ($n = 8$ to 975 independent measurements averaged per PRI level and hour, 106,433 in total). **(C)** F_q'/F_m' was correlated to PPFD, grouped according to PRI levels, and fitted to a linear model depending on PPFD (square root transformed, all measurements with associated PPFD $> 25 \mu\text{mol photons m}^{-2} \text{s}^{-1}$ were used, $n = 42,434$ to 179,152 measurements per PRI group). Chlorophyll fluorescence and spectral data was acquired by an automated light-induced fluorescence transient (LIFT) device scanning over the crop canopy. PPFD was recorded every minute by three stations distributed in the unheated glasshouse and linked to LIFT measurements done in the same minute.

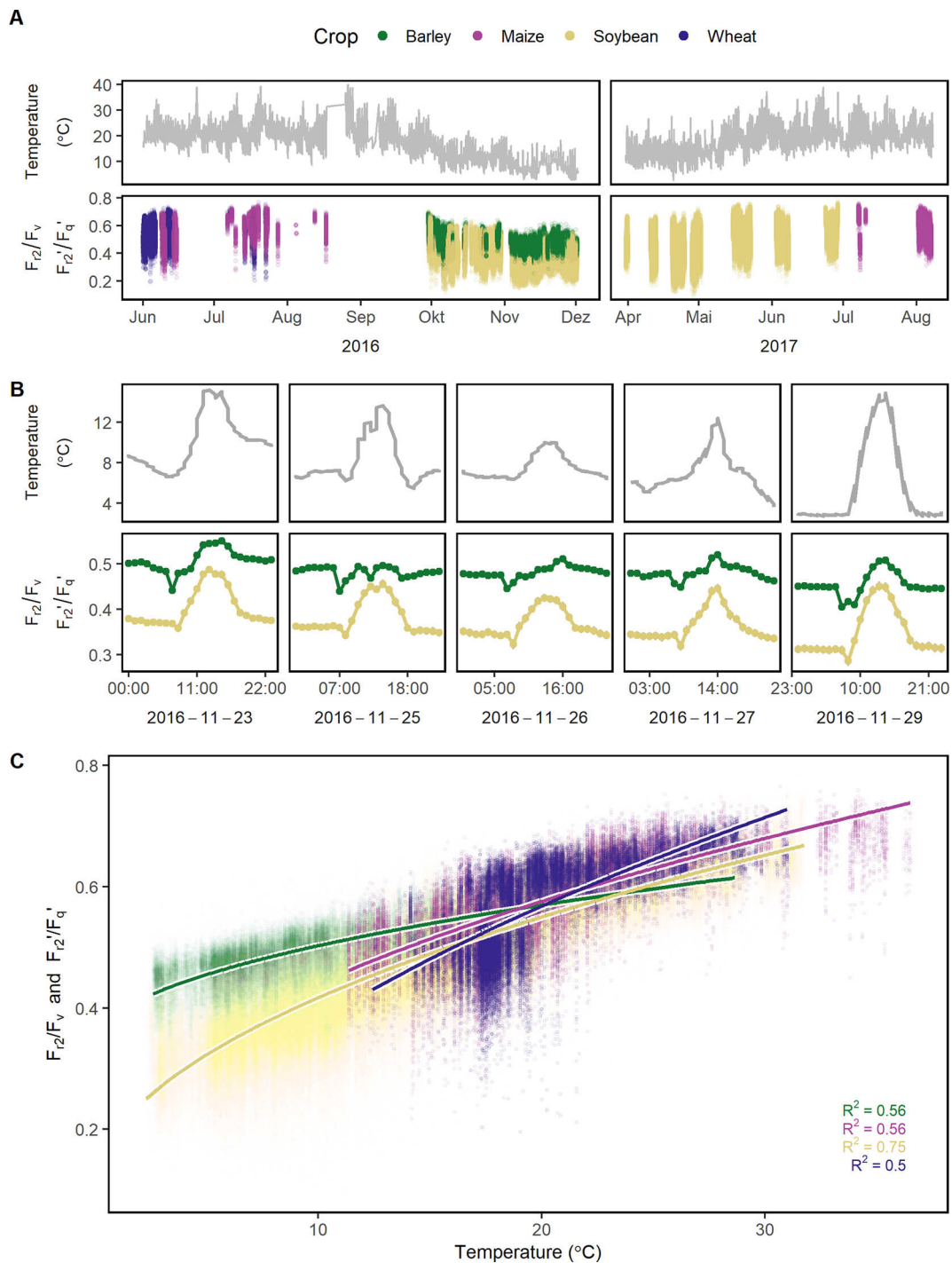


FIGURE 4 | Reoxidation efficiency 5 ms after primary quinone (Q_A) reduction (F_{r2}/F_v in the dark and F_{r2}'/F_q' in the light) of barley, maize, soybean, and wheat genotypes was monitored under a fluctuating environment over two seasons in high time resolution. **(A)** Temperature fluctuation together with the dynamic F_{r2}/F_v and F_{r2}'/F_q' of the four crop species is shown over the two growing seasons ($n = 778,224$, acquired from May 2016 to August 2017). **(B)** Temperature and F_{r2}/F_v (respective F_{r2}'/F_q') are shown in a subset of diurnal measurements within 1 week to illustrate the strong interaction between the parameters. F_{r2}/F_v and F_{r2}'/F_q' were grouped according to crop species to reveal the strong effect of the different species. Gray error bars show 95% confidence interval ($n = 58$ to 171 independent measurements averaged per crop species and hour, in total = 30,704). **(C)** F_{r2}/F_v and F_{r2}'/F_q' were correlated to temperature and fitted to a linear model depending on temperature (temperature was square root transformed, all measurements were used, $n = 33,902$ to 604,857 measurements per crop species). Chlorophyll fluorescence data was acquired by an automated light-induced fluorescence transient (LIFT) device scanning over the crop canopy. Temperature was recorded every minute by three stations distributed in the unheated glasshouse and linked to LIFT measurements done in the same minute.

TABLE 1 | Reoxidation efficiency 5 ms after primary quinone (Q_A) reduction (F_{r2}/F_v in the dark and F_{r2}'/F_q' in the light) measured in four crop species over two seasons in an unheated glasshouse was analyzed using a linear model ($n = 760,874$ measurements). Depending factors were temperature (including a square root term), time point of the measurement (month, date, and hour), crop species, genotype, plot, and days after sowing (DAS). Descriptors of the linear models are degree of freedom (Df), sum of squares, ratio of mean squares, and mean squares error (F value) and the explained sum of squares per factor (explained variance) in percentage.

	Df	Sum squares	Mean squares	F value	Explained variance (%)
Temperature	1	4,858.15	4,858.15	2,942,365	67.2
Residuals	760,640	1,255.9	0	NA	17.4
Month	12	366.97	30.58	18,521.5	5.1
Crop	2	361.88	180.94	109,587.8	5
Hour	23	206.15	8.96	5,428.6	2.9
Date	123	78.87	0.64	388.3	1.1
Genotype	24	53.54	2.23	1,351.2	0.7
Plot	46	21.07	0.46	277.4	0.3
DAS	1	17.22	17.22	10,431.2	0.2
Temperature ^{0.5}	1	12.09	12.09	7,322.7	0.2

Influence of Canopy Structure, Plant Height, and Leaf Angle

In order to estimate the variance introduced by canopy structure, soybean leaves were fixed perpendicular to the LIFT lens. At noon and night, LIFT signal was not significantly affected by changes of the measuring distance within 150 mm (**Supplementary Figure 7**). The effect of the measuring distance ranging from 750 to 1,200 mm on F_v/F_m and F_{r2}/F_v accounted for about 1.4 and 19.3% of the variance during night measurements, respectively (**Supplementary Table 5**). In contrast, leaf angle (or canopy structure) affected F_v/F_m more strongly (23.6% of explained variance) than F_{r2}/F_v (2.2% of explained variance). At noon, the explained variance of F_q'/F_m' and F_{r2}'/F_q' for leaf angle was not bigger than 8% (**Supplementary Table 6**). Regarding PRI, leaf angle accounted for 22.7% of explained variance representing canopy structure. In summary, photosynthesis, specifically regulation of F_q'/F_m' and F_{r2}'/F_q' in response to a fluctuating environment was quantified and related to environmental factors and canopy structure.

DISCUSSION

Based on diurnal and seasonal ChlF data from different crop species and genotypes, a unique dataset was collected to identify, quantify, and model photosynthesis x environmental interactions under semi-field conditions. F_v/F_m and F_q'/F_m' correlated with PPFD but not significantly with temperature. Therefore, screening for this trait detects light-use efficient genotypes at the level of PSII charge separation but misses the photosynthetic response to temperature. In contrast, F_{r2}/F_v and F_{r2}'/F_q' provided information about genotype specific differences in acclimation to temperature. In general, the responses to temperature and PPFD from lab conditions in *Arabidopsis* to fluctuating environmental conditions in the four different crop species were consistent in their trends but differed in the complexity of the interactions.

Temperature Tolerance of Electron Transport

For the first time, F_{r2}/F_v and F_{r2}'/F_q' were quantified under fluctuating semi-field conditions and their interactions with

the environment was analyzed. F_{r2}/F_v and F_{r2}'/F_q' were highly dependent on temperature pointing toward limitations of electron transport in the cold. Under cold conditions, electron transport depends on the membrane fluidity, which is maintained by the fatty acid composition (Upchurch, 2008; Liu et al., 2013). Electron transport between PSII and PSI acclimates to different growth temperatures which was shown by measurements of Q_A^- reoxidation and PSI primary donor (P700) reduction (Yamasaki et al., 2002). Exposure to cold of non-acclimated plants resulted in a severe loss of thylakoid membrane function and decreased NPQ capacity in rice plants (Suzuki et al., 2011). The efficiency to reduce the electron transport chain downstream of Q_A was reported to be increased after six nights of dark chilling compared to the control (Van Heerden et al., 2003). In general, exposure to cold of non-acclimated plants resulted in a severe loss of thylakoid membrane function, decreased reoxidation efficiency of Q_A^- , and limited electron transport and carboxylation rate (Yamori et al., 2008; Suzuki et al., 2011; Krüger et al., 2014). This probably explains the close relationship of F_{r2}/F_v and F_{r2}'/F_q' to temperature which we found under controlled (**Figure 1D**) and fluctuating conditions (**Figure 4C**). F_{r2}'/F_q' seemed to reflect the capacity of electron transport from Q_A through PQ pool toward cytochrome *b₆f* and PSI complex. In the light-adapted state, F_{r1}'/F_q' and F_{r2}'/F_q' were highly correlated indicating a continuous electron transport (**Supplementary Figure 3**). In agreement, a gradual decrease of the ChlF relaxation curve was observed in light-adapted leaves under controlled conditions (Keller et al., 2019). The changes in the ratio between F_{r1}'/F_q' and F_{r2}'/F_q' according to the time of the day were probably related to the diurnal temperature pattern. Ratio changes in the morning seemed to represent the acclimation of the photosynthetic machinery to light visible as temporary decrease in F_{r2}'/F_q' (**Figure 4B**). This transition was also observed under lab conditions upon illumination of dark-adapted leaves (Keller et al., 2019). In photosynthetic models, the response to temperature is commonly included as a constant (Bernacchi et al., 2001; Yamori et al., 2014). Under fluctuating environmental conditions, F_{r2}/F_v and F_{r2}'/F_q' could improve these models exchanging the constant by a genotypic specific variable responding to temperature at the level of electron transport.

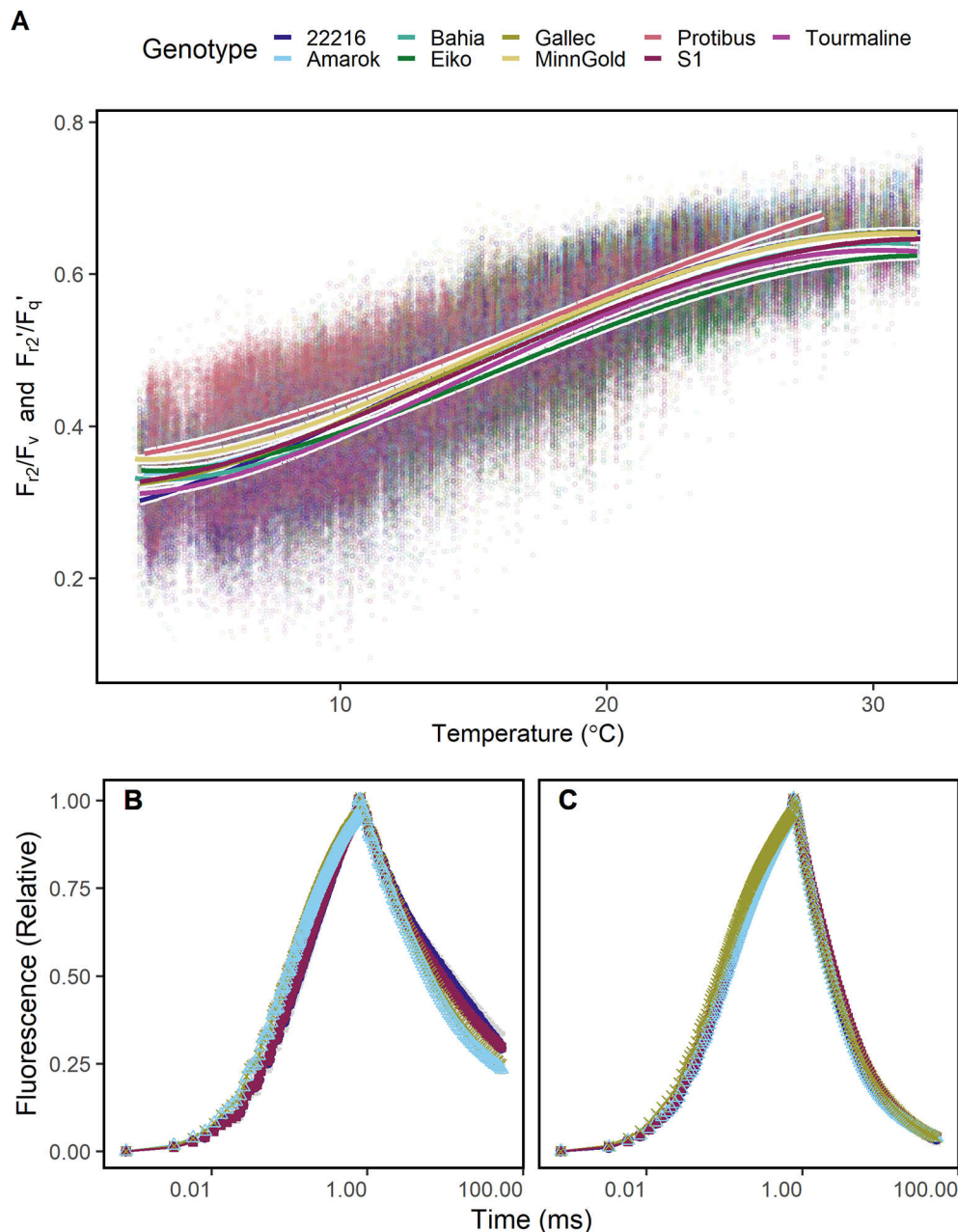


FIGURE 5 | Chlorophyll fluorescence transients were measured in soybean canopies of different genotypes over two seasons under fluctuating conditions. **(A)** Efficiency of electron transport 5 ms after reduction of primary quinone (Q_A) (F_2/F_v in the dark, F_2'/F_q' in the light) of soybean genotypes differing in cold tolerance are shown. F_2/F_v and F_2'/F_q' were fitted to a linear model depending on temperature (including a square root and a squared temperature term). **(B)** A contrasting subset of chlorophyll fluorescence transients of genotypes 22216, Amarok, Gallec, and S1 at 4°C and **(C)** 20°C is shown. F_2/F_v and F_2'/F_q' calculated from these data are shown in **Supplementary Figure 5**. For each temperature level, measurements were selected from October and November 2016 which had data recorded at the indicated temperature ($\pm 0.5^{\circ}\text{C}$) between noon and dawn. Error bars show 95% confidence interval of the mean ($n = 33$ to 161 measurements). Genotype Amarok and Gallec are breed for cold tolerance. Light-induced fluorescence transient (LIFT) method was used with fast repetition rate flash from about 1 m distance scanning over the crop canopy. Temperature was recorded every minute by three stations distributed in the unheated glasshouse and linked to LIFT measurements done in the same minute.

The detected temperature tolerance of photosynthetic electron transport varied between species and genotypes (**Figure 5A**). In general, the minimum temperature required for growth is 5°C (Körner, 2016). The cold tolerant genotype Amarok

showed higher F_2/F_v (respective F_2'/F_q') than the cold sensitive genotypes 22216 and S1 at low temperature. This tolerance of electron transport to low temperature may be related to adjusted membrane composition or general limitations at CO_2

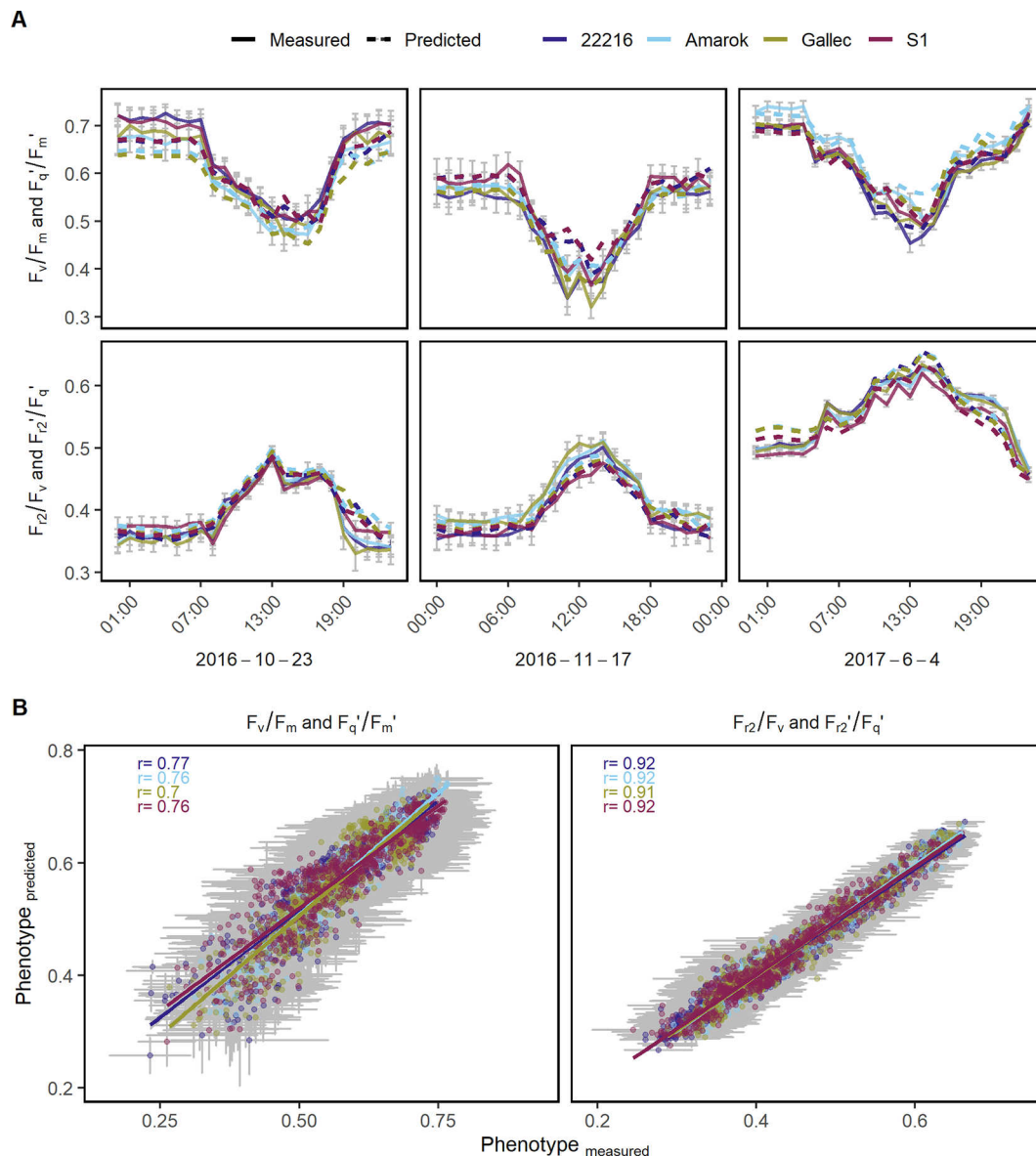


FIGURE 6 | Chlorophyll fluorescence parameters were used to model genotype x environment interactions of different soybean genotypes. **(A)** Quantum efficiency of the photosystem II (F_v/F_m in the dark and F_q'/F_m' in the light) and the efficiency of electron transport 5 ms after reduction of primary quinone (Q_A) (F_{22}/F_v in the dark, F_{22}'/F_q' in the light) at three random dates with measured (full line) and modeled (dashed line) values are shown. **(B)** Predicted and measured values for both photosynthetic parameters were correlated to each other in order to assess the model accuracy. Measurements of 48 days were used to train the model using Lasso regression ($n = 284,662$). Photosynthetic performance over the remaining 47 days was predicted and validated ($n = 295,885$). Predicted and measured values were averaged per genotype, day and hour. Error bars show the 95% confidence interval. The λ value derived through internal cross-validation on the training set was 1.14285×10^{-5} and 3.626669×10^{-5} for F_v/F_m and F_{22}/F_v , respectively. For the Lasso model coefficients see **Supplementary Table 4**.

fixation (Liu et al., 2013; Yamori et al., 2014; Pignon et al., 2019). The remaining cold tolerant genotypes, Tourmaline and Gallec, showed intermediate response indicating different cold tolerance mechanisms in soybean (Gass et al., 1996; Yamori et al., 2010). The potential to detect cold tolerance *via* the analysis of electron transport kinetics was also demonstrated earlier under lab conditions (Strauss et al., 2006; Krüger et al., 2014). We conclude that F_{22}/F_v and F_{22}'/F_q' represent efficiency of electron transport beyond Q_A reflecting membrane fluidity

and composition, and therefore contributes to the temperature tolerance at a given temperature.

Photosynthetic Interactions With Light Intensity and Canopy Architecture

In steady-state conditions, F_q'/F_m' is tightly linked to electron transport and CO_2 assimilation (Genty et al., 1989; Niyogi et al., 1998; Von Caemmerer, 2000). Under natural conditions, F_v/F_m

F_m and F_q'/F_m' follow a diurnal pattern (Adams and Demmig-Adams, 1995; Ribeiro et al., 2004; Pieruschka et al., 2008; Moura dos Santos et al., 2013; Ruiz-Vera et al., 2015). Similar results, but with higher spatio-temporal resolution over the whole seasons, were presented in this study (Figure 3A). The response of F_q'/F_m' to light measured under fluctuating semi-field conditions was almost linear (Figure 3C and Supplementary Table 1). It did not fit the response measured under controlled steady-state conditions (Figure 1B). In agreement, the curvature factor and the light saturation point were reported to be reduced under natural light conditions compared to control conditions probably caused by higher NPQ levels (Rascher et al., 2000; Jia et al., 2013; Meacham et al., 2017). In relation to that, the response of F_q'/F_m' to temperature was negligible under fluctuating conditions in contrast to lab conditions (Supplementary Table 1). The decrease of F_q'/F_m' under cold stress was associated with the inhibition of PSII reaction centers and their repair mechanism (Murata et al., 2007). Cold acclimation resulted in slower decrease of F_v/F_m after exposure to 4°C in control leaves compared to cold-hardened leaves (Streb et al., 1999). This could explain the small effect of temperature on F_q'/F_m' under fluctuating conditions allowing cold acclimation compared to lab conditions. Comparing fluctuating with controlled conditions, we conclude that the response of F_q'/F_m' to light intensity was slightly modified by higher NPQ levels while the response to temperature was minimized by cold acclimation.

Besides PPFD, F_q'/F_m' on canopy level was related to PRI in all four species examined in this study (Figure 3C). PRI is mainly linked to the xanthophyll cycle and therefore sensitive to NPQ changes and various other stress responses (Prasad et al., 2006; Garbulsky et al., 2011; Zhang et al., 2016). It explains the close relationship of PRI and F_q'/F_m' described in a recent meta-analysis (Sukhova and Sukhov, 2018). However, scans of natural crop canopy showed additionally a high variability in NDVI (e.g., Supplementary Figure 2). The NDVI is known to correlate highly with vegetation productivity, hence, we would not expect a high variability within one plot (Gamon et al., 1992; Ji and Peters, 2003). This variability could be explained with the observation that PRI as well as NDVI vary with canopy structure (Barton and North, 2001; Rascher et al., 2015; Cordon et al., 2016). Canopy structure affects physiological processes directly, e.g., the leaf angle distribution affects the light penetration into the canopy leading to variation in F_q'/F_m' and NPQ. In addition, F_q'/F_m' values differed in the upper compared to the lower canopy and were affected by steep leaf angles (Rascher and Pieruschka, 2008; Wyber et al., 2018). Our data support this conclusion: variability in F_q'/F_m' , NPQ, and PRI were higher in leaves with natural orientation than in leaves with a fixed leaf angle (Supplementary Figure 7). The leaf angle explained more of the variation in PRI than in F_q'/F_m' indicating an additional influence of canopy structure to PRI (Supplementary Table 6). Similarly, the correlations between PRI and F_q'/F_m' decreased when measured on canopy compared to leaf level (Sukhova and Sukhov, 2018). These findings indicate a combination of NPQ level and canopy structure expressed in F_q'/F_m' and PRI. The variability in F_q'/F_m' on canopy level describes plant

performance in the field more realistic than measurements on selected leaves or leaf segments (Evans, 2013; Niinemets et al., 2015). In conclusion, the variability of F_v/F_m and F_q'/F_m' combines physiological and structural canopy information without the requirement to select leaves for measurement under steady-state conditions.

Prediction of Photosynthesis in a Fluctuating Environment

Photosynthetic genotype x environment interactions were modeled over the entire growing season based on environmental parameters and training data from another season (Supplementary Figure 6). The accurate prediction across seasons (Pearson correlation coefficient between 0.44 and 0.84) indicated that our modeling is valid for a wide range of environmental conditions confirming the identified predictive parameters. Based on these models, the total amount of electron transported through a season for a specific genotype is possible to estimate without having measurement data from that season. This has potential application in crop growth models to increase the prediction of plant performance in untested environments (van Eeuwijk et al., 2019; Voss-Fels et al., 2019). The LIFT method is directly applicable in high-throughput field phenotyping requiring about 30 s to scan 1 m plot. A few diurnal measurements over the season seem to be sufficient to model the full photosynthetic response. Different development stages were probably represented in our models *via* seasonal changes of reflectance indices such as NDVI (Condorelli et al., 2018). In the soybean data of 2017, development stage represented by DAS was correlated to NDVI with a Pearson correlation coefficient of 0.63 (data not shown). Further research is needed to increase the model prediction accuracies and to gain more detailed knowledge about driving factors of photosynthesis in the field. Based on the detected environmental interactions, the modeling and estimation of photosynthetic performance at the genotype level over entire growing seasons is possible.

CONCLUSIONS

Diurnal and seasonal fluctuation of photosynthesis at canopy level was successfully quantified using ChlF measurements in high-throughput. F_v/F_m and F_q'/F_m' and the newly established ChlF parameters F_{r2}/F_v and F_{r2}/F_q' were able to detect photosynthetic acclimation under fluctuating semi-field conditions. F_q'/F_m' provided the quantum efficiency at the level of PSII and was mainly determined by PPFD. In contrast, F_{r2}'/F_q' was rather independent of PPFD and reflected efficiency of electron transport beyond Q_A . F_{r2}/F_v and F_{r2}/F_q' showed a high sensitivity to temperature identifying electron transport limitations at low temperature when F_v/F_m was not affected. The automated scans allowed a high spatio-temporal resolution of the data. It enabled the analysis of several genotypes regarding not only means under steady-state conditions but also their dynamic interaction with environmental factors. Autonomous monitoring of photosynthesis x environment interactions

under natural conditions as well as their predictions over entire growing seasons has great potential in plant physiology and breeding applications.

DATA AVAILABILITY STATEMENT

The datasets generated and analyzed for this study can be found under the DOI 10.5281/zenodo.3260253.

AUTHOR CONTRIBUTIONS

BK, SM, OM, UR, and RP designed the study. BK, AS, TK, and OM carried out the experiments, AS, OM, RP, SM, and UR contributed materials and advice. BK and SM wrote the manuscript with contributions from TK, UR, and OM.

FUNDING

German-Plant-Phenotyping Network funded by the German Federal Ministry of Education and Research (project identification number: 031A053).

REFERENCES

- Adams, W. W., and Demmig-Adams, B. (1995). The xanthophyll cycle and sustained thermal energy dissipation activity in *Vinca minor* and *Euonymus kiautschovicus* in winter. *Plant Cell Environ.* 18, 117–127. doi: 10.1111/j.1365-3040.1995.tb00345.x
- Adams, W. W. III, Zarter, C. R., Mueh, K. E., Amiard, V., and Demmig-Adams, B. (2006). Energy dissipation and photoinhibition: a continuum of photoprotection, in *Photoprotection, Photoinhibition, Gene Regulation, and Environment*. Eds. Demmig-Adams, W. W., Adams, A. K., and Mattoo, B. (Dordrecht: Springer Netherlands), 49–64. doi: 10.1007/1-4020-3579-9_5
- Baker, N. R. (2008). Chlorophyll fluorescence: A probe of photosynthesis in vivo. *Annu. Rev. Plant Biol.* 59, 89–113. doi: 10.1146/annurev-arplant.59.032607.092759
- Barton, C. V. M., and North, P. R. J. (2001). Remote sensing of canopy light use efficiency using the photochemical reflectance index: Model and sensitivity analysis. *Remote Sens. Environ.* 78, 264–273. doi: 10.1016/S0034-4257(01)00224-3
- Bernacchi, C., Singaas, E., Pimentel, C., Portis, A., and Long, S. (2001). Improved temperature response functions for models of Rubisco-limited photosynthesis. *Plant Cell Environ.* 24, 253–259. doi: 10.1111/j.1365-3040.2001.00668.x
- Bezouw, R. F. H. M., van Keurentjes, J. J. B., Harbinson, J., and Aarts, M. G. M. (2019). Converging phenomics and genomics to study natural variation in plant photosynthetic efficiency. *Plant J.* 97, 112–133. doi: 10.1111/tpj.14190
- Bundessortenamt. (2013). Beschreibende Sortenliste - Sortenliste Getreide, Mais, Öl- und Faserpflanzen, Leguminosen, Rüben, Zwischenfrüchte (Hannover).
- Campbell, B. W., Mani, D., Curtin, S. J., Slattery, R. A., Michno, J.-M., Ort, D. R., et al. (2015). Identical substitutions in magnesium chelatase paralogs result in chlorophyll-deficient soybean mutants. *G3 Genes Genomes Genetics* 5, 123–131. doi: 10.1534/g3.114.015255
- Condorelli, G. E., Maccaferri, M., Newcomb, M., Andrade-Sanchez, P., White, J. W., French, A. N., et al. (2018). Comparative aerial and ground based high throughput phenotyping for the genetic dissection of NDVI as a proxy for drought adaptive traits in durum wheat. *Front. Plant Sci.* 9, 893. doi: 10.3389/fpls.2018.00893
- Cordon, G., Lagorio, M. G., and Paruelo, J. M. (2016). Chlorophyll fluorescence, photochemical reflective index and normalized difference vegetative index

ACKNOWLEDGMENTS

Soybean, wheat and maize lines were kindly provided by Agroscope Changins, Switzerland, EMBRAPA Brasília, Brazil, and IPK Gatersleben, Germany, respectively. We would like to thank Stefan Thomas for allowing measurements in the barley experiment. Many thanks go to the Miniplot facility team on the campus Klein-Altendorf, especially Ines Munoz-Fernandez, Karl-Josef Wiesel and Hubert Kühn. Furthermore, we would like to acknowledge Beate Uhlig, Marcel Schneider, Katharina Wolter-Heinen and Christian Jungmann to ensure optimal plant growth conditions in the greenhouses. Part of this work was performed within the German-Plant-Phenotyping Network which is funded by the German Federal Ministry of Education and Research (project identification number: 031A053). This work is part of the doctoral thesis of Beat Keller (2018) done at the Forschungszentrum Jülich and University of Bonn.

SUPPLEMENTARY MATERIAL

The Supplementary Material for this article can be found online at: <https://www.frontiersin.org/articles/10.3389/fpls.2019.01482/full#supplementary-material>

- during plant senescence. *J. Plant Physiol.* 199, 100–110. doi: 10.1016/j.jplph.2016.05.010
- Croce, R. (2015). PsbS is the plants' pick for sun protection. *Nat. Struct. Mol. Biol.* 22, 650–652. doi: 10.1038/nsmb.3079
- D'Odorico, P., Emmel, C., Revill, A., Liebisch, F., Eugster, W., and Buchmann, N. (2019). Vertical patterns of photosynthesis and related leaf traits in two contrasting agricultural crops. *Funct. Plant Biol.* 46, 213–227. doi: 10.1071/FP18061
- Dahal, K., Kane, K., Gadapati, W., Webb, E., Savitch, L. V., Singh, J., et al. (2012). The effects of phenotypic plasticity on photosynthetic performance in winter rye, winter wheat and Brassica napus. *Physiol. Plant* 144, 169–188. doi: 10.1111/j.1399-3054.2011.01513.x
- Dash, J., and Curran, P. J. (2004). The MERIS terrestrial chlorophyll index. *Int. J. Remote Sens.* 25, 5403–5413. doi: 10.1080/0143116042000274015
- de Wijn, R., and van Gorkom, H. J. (2001). Kinetics of Electron Transfer from QA to QB in Photosystem II. *Biochem. (Mosc.)* 40, 11912–11922. doi: 10.1021/bi010852r
- Demmig-Adams, B., Cohu, C. M., Muller, O., and Adams, W. W. (2012). Modulation of photosynthetic energy conversion efficiency in nature: from seconds to seasons. *Photosynth. Res.* 113, 75–88. doi: 10.1007/s11120-012-9761-6
- Ensminger, I., Busch, E., and Huner, N. P. A. (2006). Photostasis and cold acclimation: sensing low temperature through photosynthesis. *Physiol. Plant* 126, 28–44. doi: 10.1111/j.1399-3054.2006.00627.x
- Evans, J. R., and Poorter, H. (2001). Photosynthetic acclimation of plants to growth irradiance: the relative importance of specific leaf area and nitrogen partitioning in maximizing carbon gain. *Plant Cell Environ.* 24, 755–767. doi: 10.1046/j.1365-3040.2001.00724.x
- Evans, J. R. (2013). Improving Photosynthesis. *Plant Physiol.* 162, 1780–1793. doi: 10.1104/pp.113.219006
- Fiorani, F., and Schurr, U. (2013). Future scenarios for plant phenotyping. *Annu. Rev. Plant Biol.* 64, 267–291. doi: 10.1146/annurev-arplant-050312-120137
- Flood, P. J., Kruijer, W., Schnabel, S. K., van der Schoor, R., Jalink, H., Snel, J. F. H., et al. (2016). Phenomics for photosynthesis, growth and reflectance in *Arabidopsis thaliana* reveals circadian and long-term fluctuations in heritability. *Plant Methods* 12, 14. doi: 10.1186/s13007-016-0113-y
- Frampton, W. J., Dash, J., Watmough, G., and Milton, E. J. (2013). Evaluating the capabilities of Sentinel-2 for quantitative estimation of biophysical variables

- in vegetation. *ISPRS J. Photogramm. Remote Sens.* 82, 83–92. doi: 10.1016/j.isprsjprs.2013.04.007
- Frascaroli, E. (2018). Breeding Cold-Tolerant Crops, in *Cold Tolerance in Plants: Physiological, Molecular and Genetic Perspectives*. Eds. Wani, V., and Herath, S. H. (Cham: Springer International Publishing), 159–177. doi: 10.1007/978-3-030-01415-5_9
- Friedman, J., Hastie, T., and Tibshirani, R. (2010). Regularization paths for generalized linear models via coordinate descent. *J. Stat. Software* 33, 1–22. doi: 10.18637/jss.v033.i01
- Gamon, J. A., Peñuelas, J., and Field, C. B. (1992). A narrow-waveband spectral index that tracks diurnal changes in photosynthetic efficiency. *Remote Sens. Environ.* 41, 35–44. doi: 10.1016/0034-4257(92)90059-S
- Garbulsky, M. F., Peñuelas, J., Gamon, J., Inoue, Y., and Filella, I. (2011). The photochemical reflectance index (PRI) and the remote sensing of leaf, canopy and ecosystem radiation use efficiencies: A review and meta-analysis. *Remote Sens. Environ.* 115, 281–297. doi: 10.1016/j.rse.2010.08.023
- Gass, T., Schori, A., Fossati, A., Soldati, A., and Stamp, P. (1996). Cold tolerance of soybean (*Glycine max* (L.) Merr.) during the reproductive phase. *Eur. J. Agron.* 5, 71–88. doi: 10.1016/S1161-0301(96)02011-4
- Genty, B., Briantais, J.-M., and Baker, N. R. (1989). The relationship between the quantum yield of photosynthetic electron transport and quenching of chlorophyll fluorescence. *Biochim. Biophys. Acta BBA - Gen. Subj.* 990, 87–92. doi: 10.1016/S0304-4165(89)80016-9
- Hüner, N. P. A., Bode, R., Dahal, K., Busch, F. A., Possmayer, M., Szyszka, B., et al. (2012). Shedding some light on cold acclimation, cold adaptation, and phenotypic plasticity. *Botany* 91, 127–136. doi: 10.1139/cjb-2012-0174
- Hecht, V. L., Temperton, V. M., Nagel, K. A., Rascher, U., and Postma, J. A. (2016). Sowing Density: A neglected factor fundamentally affecting root distribution and biomass allocation of field grown spring barley (*Hordeum Vulgare* L.). *Front. Plant Sci.* 7, 944. doi: 10.3389/fpls.2016.00944
- Huner, N. P. A., Öquist, G., Hurry, V. M., Krol, M., Falk, S., and Griffith, M. (1993). Photosynthesis, photoinhibition and low temperature acclimation in cold tolerant plants. *Photosynth. Res.* 37, 19–39. doi: 10.1007/BF02185436
- Huner, N. P. A., Öquist, G., and Sarhan, F. (1998). Energy balance and acclimation to light and cold. *Trends Plant Sci.* 3, 224–230. doi: 10.1016/S1360-1385(98)01248-5
- Jansen, M., Gilmer, F., Biskup, B., Nagel, K. A., Rascher, U., Fischbach, A., et al. (2009). Simultaneous phenotyping of leaf growth and chlorophyll fluorescence via GROWSCREEN FLUORO allows detection of stress tolerance in *Arabidopsis thaliana* and other rosette plants. *Funct. Plant Biol.* 36, 902–914. doi: 10.1071/FP09095
- Ji, L., and Peters, A. J. (2003). Assessing vegetation response to drought in the northern Great Plains using vegetation and drought indices. *Remote Sens. Environ.* 87, 85–98. doi: 10.1016/S0034-4257(03)00174-3
- Jia, H., Foerster, B., Chow, W. S., Pogson, B. J., and Osmond, C. B. (2013). Decreased photochemical efficiency of photosystem II following sunlight exposure of shade-grown leaves of avocado: because of, or in spite of, two kinetically distinct xanthophyll cycles? *Plant Physiol.* 161, 836–852. doi: 10.1104/pp.112.209692
- Körner, C., Körner, C. (2016). Plant adaptation to cold climates. *F1000Research* 5. doi: 10.12688/f1000research.9107.1
- Kaiser, E., Matsubara, S., Harbinson, J., Heuvelink, E., and Marcelis, L. F. M. (2018a). Acclimation of photosynthesis to lightflecks in tomato leaves: interaction with progressive shading in a growing canopy. *Physiol. Plant.* 162, 506–517. doi: 10.1111/ppl.12668
- Kaiser, E., Morales, A., and Harbinson, J. (2018b). Fluctuating light takes crop photosynthesis on a rollercoaster ride. *Plant Physiol.* 176, 977. doi: 10.1104/pp.17.01250
- Kalaji, H. M., Jajoo, A., Oukarroum, A., Brestic, M., Zivcak, M., Samborska, I. A., et al. (2016). Chlorophyll a fluorescence as a tool to monitor physiological status of plants under abiotic stress conditions. *Acta Physiol. Plant* 38, 102. doi: 10.1007/s11738-016-2113-y
- Kalaji, H. M., Schansker, G., Brestic, M., Bussotti, F., Calatayud, A., Ferroni, L., et al. (2017). Frequently asked questions about chlorophyll fluorescence, the sequel. *Photosynth. Res.* 132, 13–66. doi: 10.1007/s11120-016-0318-y
- Keller, B., Vass, I., Matsubara, S., Paul, K., Jedmowski, C., Pieruschka, R., et al. (2019). Maximum fluorescence and electron transport kinetics determined by light-induced fluorescence transients (LIFT) for photosynthesis phenotyping. *Photosynth. Res.* 140, 221–233. doi: 10.1007/s11120-018-0594-9
- Keller, B. (2018). Analyzing photosynthetic performance in natural fluctuating environment using light-induced fluorescence transient (LIFT) method in high-throughput. *Dissertation. Univ. Bonn*.
- Kolber, Z. S., Prasil, O., and Falkowski, P. G. (1998). Measurements of variable chlorophyll fluorescence using fast repetition rate techniques: defining methodology and experimental protocols. *Biochim. Biophys. Acta-Bioenerg.* 1367, 88–106. doi: 10.1016/S0005-2728(98)00135-2
- Kono, M., and Terashima, I. (2014). Long-term and short-term responses of the photosynthetic electron transport to fluctuating light. *J. Photochem. Photobiol. B* 137, 89–99. doi: 10.1016/j.jphotobiol.2014.02.016
- Krüger, G. H. J., De Villiers, M. F., Strauss, A. J., de Beer, M., van Heerden, P. D. R., Maldonado, R., et al. (2014). Inhibition of photosystem II activities in soybean (*Glycine max*) genotypes differing in chilling sensitivity. *South Afr. J. Bot.* 95, 85–96. doi: 10.1016/j.sajb.2014.07.010
- Kromdijk, J., Glowacka, K., Leonelli, L., Gabilly, S. T., Iwai, M., Niyogi, K. K., et al. (2016). Improving photosynthesis and crop productivity by accelerating recovery from photoprotection. *Science* 354, 857. doi: 10.1126/science.aai8878
- Lazár, D. (2015). Parameters of photosynthetic energy partitioning. *J. Plant Physiol.* 175, 131–147. doi: 10.1016/j.jplph.2014.10.021
- Liu, X. Y., Teng, Y. B., Li, B., and Meng, Q. W. (2013). Enhancement of low-temperature tolerance in transgenic tomato plants overexpressing Lefad7 through regulation of trienoic fatty acids. *Photosynthetica* 51, 238–244. doi: 10.1007/s11099-013-0014-5
- Liu, Y., Dang, P., Liu, L., and He, C. (2019). Cold acclimation by the CBF-COR pathway in a changing climate: Lessons from *Arabidopsis thaliana*. *Plant Cell Rep.* 38, 511–519. doi: 10.1007/s00299-019-02376-3
- Meacham, K., Sirault, X., Quick, W. P., von Caemmerer, S., and Furbank, R. (2017). Diurnal Solar Energy Conversion and Photoprotection in Rice Canopies. *Plant Physiol.* 173, 495–508. doi: 10.1104/pp.16.01585
- Mishra, A., Heyer, A. G., and Mishra, K. B. (2014). Chlorophyll fluorescence emission can screen cold tolerance of cold acclimated *Arabidopsis thaliana* accessions. *Plant Methods* 10, 38. doi: 10.1186/1746-4811-10-38
- Mitchell, R. A. C., and Barber, J. (1986). Adaptation of photosynthetic electron-transport rate to growth temperature in pea. *Planta* 169, 429–436. doi: 10.1007/BF00392141
- Moura dos Santos, C., Verissimo, V., Filho, H. C., de, L. W., Ferreira, V. M., da S., P. G., et al. (2013). Seasonal variations of photosynthesis, gas exchange, quantum efficiency of photosystem II and biochemical responses of *Jatropha curcas* L. grown in semi-humid and semi-arid areas subject to water stress. *Ind. Crops Prod.* 41, 203–213. doi: 10.1016/j.indcrop.2012.04.003
- Murakami, Y., Tsuyama, M., Kobayashi, Y., Kodama, H., and Iba, K. (2000). Trienoic fatty acids and plant tolerance of high temperature. *Science* 287, 476–479. doi: 10.1126/science.287.5452.476
- Murata, N., Takahashi, S., Nishiyama, Y., and Allakhverdiev, S. I. (2007). Photoinhibition of photosystem II under environmental stress. *Biochim. Biophys. Acta BBA - Bioenerg.* 1767, 414–421. doi: 10.1016/j.bbabi.2006.11.019
- Murchie, E. H., Kefauver, S., Araus, J. L., Muller, O., Rascher, U., Flood, P. J., et al. (2018). Measuring the dynamic photosynthetic. *Ann. Bot.* 122, 207–220. doi: 10.1093/aob/mcy087
- Niinemets, Ü., Keenan, T. F., and Hallik, L. (2015). A worldwide analysis of within-canopy variations in leaf structural, chemical and physiological traits across plant functional types. *New Phytol.* 205, 973–993. doi: 10.1111/nph.13096
- Niyogi, K. K., Grossman, A. R., and Björkman, O. (1998). *Arabidopsis* mutants define a central role for the xanthophyll cycle in the regulation of photosynthetic energy conversion. *Plant Cell* 10, 1121. doi: 10.1105/tpc.10.7.1121
- Noctor, G., Rees, D., Young, A., and Horton, P. (1991). The relationship between zeaxanthin, energy-dependent quenching of chlorophyll fluorescence, and trans-thylakoid pH gradient in isolated chloroplasts. *Biochim. Biophys. Acta BBA - Bioenerg.* 1057, 320–330. doi: 10.1016/S0005-2728(05)80143-4
- Osmond, B., Chow, W. S., Wyber, R., Zavafer, A., Keller, B., Pogson, B. J., et al. (2017). Relative functional and optical absorption cross sections of PSII and other photosynthetic parameters monitored in situ, at a distance with a time resolution of a few seconds, using a prototype Light Induced Fluorescence Transient (LIFT) device. *Funct. Plant Biol.* 44, 985–1006. doi: 10.1071/FP17024

- Petrrouleas, V., and Crofts, A. (2005). The Iron-Quinone Acceptor in *Photosystem II*. Eds. Wydrzynski, K., Satoh, J., and Freeman, T. (Netherlands: Springer), 177–206. doi: 10.1007/1-4020-4254-X_9
- Pieruschka, R., Klimov, D., Rascher, U., Kolber, Z., and Berry, J. (2008). Remote Monitoring of Photosynthetic Efficiency Using Laser Induced Fluorescence Transient (LIFT) Technique, in *Photosynthesis. Energy from the Sun*. Eds. Allen, E., Gantt, J., Golbeck, B., and Osmond, J. (Netherlands: Springer), 1539–1543. doi: 10.1007/978-1-4020-6709-9_330
- Pieruschka, R., Klimov, D., Kolber, Z. S., and Berry, J. A. (2010). Monitoring of cold and light stress impact on photosynthesis by using the laser induced fluorescence transient (LIFT) approach. *Funct. Plant Biol.* 37, 395–402. doi: 10.1071/FP09266
- Pignon, C. P., Lundgren, M. R., Osborne, C. P., and Long, S. P. (2019). Bundle sheath chloroplast volume can house sufficient Rubisco to avoid limiting C4 photosynthesis during chilling. *J. Exp. Bot.* 70, 357–365. doi: 10.1093/jxb/ery345
- Poersch-Bortolon, L. B., Scagliusi, S. M. M., Yamazaki-Lau, E., and Bodanese-Zanettini, M. H. (2016). Androgenic response of Brazilian wheat genotypes to different pretreatments of spikes and to a gelling agent. *Pesqui. Agropecuária Bras.* 51, 1839–1847. doi: 10.1590/s0100-204x2016001100006
- Prasad, A. K., Chai, L., Singh, R. P., and Kafatos, M. (2006). Crop yield estimation model for Iowa using remote sensing and surface parameters. *Int. J. Appl. Earth Obs. Geoinformation* 8, 26–33. doi: 10.1016/j.jag.2005.06.002
- Rapacz, M., Gasiór, D., Zwierzykowski, Z., Lesniewska-Bocianowska, A., Humphreys, M. W., and Gay, A. P. (2004). Changes in cold tolerance and the mechanisms of acclimation of photosystem II to cold hardening generated by anther culture of *Festuca pratensis* × *Lolium multiflorum* cultivars. *New Phytol.* 162, 105–114. doi: 10.1111/j.1469-8137.2004.01024.x
- Rapacz, M., Wolanin, B., Hura, K., and Tyrka, M. (2008). The Effects of Cold Acclimation on Photosynthetic Apparatus and the Expression of COR14b in Four Genotypes of Barley (*Hordeum vulgare*) Contrasting in their Tolerance to Freezing and High-light Treatment in Cold Conditions. *Ann. Bot.* 101, 689–699. doi: 10.1093/aob/mcn008
- Rapacz, M., Ergon, A., Höglind, M., Jørgensen, M., Jurczyk, B., Ostrem, L., et al. (2014). Overwintering of herbaceous plants in a changing climate. Still more questions than answers. *Plant Sci. Int. J. Exp. Plant Biol.* 225, 34–44. doi: 10.1016/j.plantsci.2014.05.009
- Rascher, U., and Nedbal, L. (2006). Dynamics of photosynthesis in fluctuating light - Commentary. *Curr. Opin. Plant Biol.* 9, 671–678. doi: 10.1016/j.pbi.2006.09.012
- Rascher, U., and Pieruschka, R. (2008). Spatio-temporal variations of photosynthesis: the potential of optical remote sensing to better understand and scale light use efficiency and stresses of plant ecosystems. *Precis. Agric.* 9, 355–366. doi: 10.1007/s11119-008-9074-0
- Rascher, U., Liebig, M., and Lüttge, U. (2000). Evaluation of instant light-response curves of chlorophyll fluorescence parameters obtained with a portable chlorophyll fluorometer on site in the field. *Plant Cell Environ.* 23, 1397–1405. doi: 10.1046/j.1365-3040.2000.00650.x
- Rascher, U., Alonso, L., Burkart, A., Cilia, C., Cogliati, S., Colombo, R., et al. (2015). Sun-induced fluorescence – a new probe of photosynthesis: First maps from the imaging spectrometer HyPlant. *Glob. Change Biol.* 21, 4673–4684. doi: 10.1111/gcb.13017
- Ribeiro, R., dos Santos, M., Souza, G., Machado, E., de Oliveira, R., Angelocci, L., et al. (2004). Environmental effects on photosynthetic capacity of bean genotypes. *Pesqui. Agropecuária Bras.* 39, 615–623. doi: 10.1590/S0100-204X2004000700001
- Rogers, A., Medlyn, B. E., Dukes, J. S., Bonan, G., Caemmerer, S., Dietze, M. C., et al. (2017). A roadmap for improving the representation of photosynthesis in Earth system models. *New Phytol.* 213, 22–42. doi: 10.1111/nph.14283
- Ruiz-Vera, U. M., Siebers, M. H., Drag, D. W., Ort, D. R., and Bernacchi, C. J. (2015). Canopy warming caused photosynthetic acclimation and reduced seed yield in maize grown at ambient and elevated [CO₂]. *Glob. Change Biol.* 21, 4237–4249. doi: 10.1111/gcb.13013
- Sage, R. E., and Kubien, D. S. (2007). The temperature response of C3 and C4 photosynthesis. *Plant Cell Environ.* 30, 1086–1106. doi: 10.1111/j.1365-3040.2007.01682.x
- Schickling, A., Matveeva, M., Damm, A., Schween, J. H., Wahner, A., Graf, A., et al. (2016). Combining Sun-Induced Chlorophyll Fluorescence and Photochemical Reflectance Index Improves Diurnal Modeling of Gross Primary Productivity. *Remote Sens.* 8, 574. doi: 10.3390/rs8070574
- Shrestha, S., Brueck, H., and Asch, F. (2012). Chlorophyll index, photochemical reflectance index and chlorophyll fluorescence measurements of rice leaves supplied with different N levels. *J. Photochem. Photobiol. B* 113, 7–13. doi: 10.1016/j.jphotobiol.2012.04.008
- Strauss, A. J., Krüger, G. H. J., Strasser, R. J., and Heerden, P. D. R. V. (2006). Ranking of dark chilling tolerance in soybean genotypes probed by the chlorophyll a fluorescence transient O-J-I-P. *Environ. Exp. Bot.* 56, 147–157. doi: 10.1016/j.envexpbot.2005.01.011
- Streb, P., Shang, W., and Feierabend, J. (1999). Resistance of cold-hardened winter rye leaves (*Secale cereale* L.) to photo-oxidative stress. *Plant Cell Environ.* 22, 1211–1223. doi: 10.1046/j.1365-3040.1999.00483.x
- Sukhova, E., and Sukhov, V. (2018). Connection of the Photochemical Reflectance Index (PRI) with the Photosystem II Quantum Yield and Nonphotochemical Quenching Can Be Dependent on Variations of Photosynthetic Parameters among Investigated Plants: A Meta-Analysis. *Remote Sens.* 10, 771. doi: 10.3390/rs10050771
- Suzuki, K., Ohmori, Y., and Ratel, E. (2011). High Root Temperature Blocks Both Linear and Cyclic Electron Transport in the Dark During Chilling of the Leaves of Rice Seedlings. *Plant Cell Physiol.* 52, 1697–1707. doi: 10.1093/pcp/pcr104
- Svensson, J. T., Crosatti, C., Campoli, C., Bassi, R., Stanca, A. M., Close, T. J., et al. (2006). Transcriptome Analysis of Cold Acclimation in Barley Albina and Xantha Mutants. *Plant Physiol.* 141, 257–270. doi: 10.1104/pp.105.072645
- Thomas, S., Behmann, J., Steier, A., Kraska, T., Müller, O., Rascher, U., et al. (2018). Quantitative assessment of disease severity and rating of barley cultivars based on hyperspectral imaging in a non-invasive, automated phenotyping platform. *Plant Methods* 14, 45. doi: 10.1186/s13007-018-0313-8
- Townsend, A. J., Retkute, R., Chinnathambi, K., Randall, J. W., Foulkes, J., Carmo-Silva, E., et al. (2018). Suboptimal acclimation of photosynthesis to light in wheat canopies. *Plant Physiol.* 176, 1233–1246. doi: 10.1104/pp.17.01213
- Upchurch, R. G. (2008). Fatty acid unsaturation, mobilization, and regulation in the response of plants to stress. *Biotechnol. Lett.* 30, 967–977. doi: 10.1007/s10529-008-9639-z
- van Eeuwijk, F., Bustos-Korts, D., Millet, E. J., Boer, M., Kruijer, W., Thompson, A., et al. (2019). Modelling strategies for assessing and increasing the effectiveness of new phenotyping techniques in plant breeding. *Plant Sci.* 282, 23–39. doi: 10.1016/j.plantsci.2018.06.018
- Van Heerden, P. D. R., Tsimilli-Michael, M., Krüger, G. H. J., and Strasser, R. J. (2003). Dark chilling effects on soybean genotypes during vegetative development: parallel studies of CO₂ assimilation, chlorophyll a fluorescence kinetics O-J-I-P and nitrogen fixation. *Physiol. Plant* 117, 476–491. doi: 10.1034/j.1399-3054.2003.00056.x
- Vass, I., Kirilovsky, D., and Etienne, A. L. (1999). UV-B radiation-induced donor- and acceptor-side modifications of photosystem II in the cyanobacterium *Synechocystis* sp PCC 6803. *Biochem. (Mosc.)* 38, 12786–12794. doi: 10.1021/bi991094w
- Violet-Chabrand, S., Matthews, J. S. A., Simkin, A. J., Raines, C. A., and Lawson, T. (2017). Importance of Fluctuations in Light on Plant Photosynthetic Acclimation. *Plant Physiol.* 173, 2163. doi: 10.1104/pp.16.01767
- Von Caemmerer, S. (2000). *Biochemical models of leaf photosynthesis*. Collingwood, Vic: CSIRO Publishing. doi: 10.1071/9780643103405
- Voss-Fels, K. P., Cooper, M., and Hayes, B. J. (2019). Accelerating crop genetic gains with genomic selection. *Theor. Appl. Genet.* 132, 669–686. doi: 10.1007/s00122-018-3270-8
- Wang, H., Qian, X., Zhang, L., Xu, S., Li, H., Xia, X., et al. (2018). A Method of High Throughput Monitoring Crop Physiology Using Chlorophyll Fluorescence and Multispectral Imaging. *Front. Plant Sci.* 9, 407. doi: 10.3389/fpls.2018.00407
- Warren, C., and Dreyer, E. (2006). Temperature response of photosynthesis and internal conductance to CO₂: results from two independent approaches. *J. Exp. Bot.* 57, 3057–3067. doi: 10.1093/jxb/erl067
- Wu, C., Huang, W., Yang, Q., and Xie, Q. (2015). Improved estimation of light use efficiency by removal of canopy structural effect from the photochemical reflectance index (PRI). *Agric. Ecosyst. Environ.* 199, 333–338. doi: 10.1016/j.agee.2014.10.017
- Wyber, R., Osmond, B., Ashcroft, M. B., Malenovsky, Z., and Robinson, S. A. (2018). Remote monitoring of dynamic canopy photosynthesis with high time resolution light-induced fluorescence transients. *Tree Physiol.* 38, 1302–1318. doi: 10.1093/treephys/tpx161

- Yamasaki, T., Yamakawa, T., Yamane, Y., Koike, H., Satoh, K., and Katoh, S. (2002). Temperature acclimation of photosynthesis and related changes in photosystem II electron transport in winter wheat. *Plant Physiol.* 128, 1087–1097. doi: 10.1104/pp.010919
- Yamori, W., Noguchi, K., Kashino, Y., and Terashima, I. (2008). The role of electron transport in determining the temperature dependence of the photosynthetic rate in spinach leaves grown at contrasting temperatures. *Plant Cell Physiol.* 49, 583–591. doi: 10.1093/pcp/pcn030
- Yamori, W., Noguchi, K., Hikosaka, K., and Terashima, I. (2010). Phenotypic Plasticity in Photosynthetic Temperature Acclimation among Crop Species with Different Cold Tolerances. *Plant Physiol.* 152, 388–399. doi: 10.1104/pp.109.145862
- Yamori, W., Hikosaka, K., and Way, D. A. (2014). Temperature response of photosynthesis in C3, C4, and CAM plants: temperature acclimation and temperature adaptation. *Photosynth. Res.* 119, 101–117. doi: 10.1007/s11120-013-9874-6
- Zhang, C., Filella, I., Garbulsky, M. F., and Peñuelas, J. (2016). Affecting Factors and Recent Improvements of the Photochemical Reflectance Index (PRI) for Remotely Sensing Foliar, Canopy and Ecosystemic Radiation-Use Efficiencies. *Remote Sens.* 8, 677. doi: 10.3390/rs8090677
- Zuther, E., Juszczak, I., Ping Lee, Y., Baier, M., and Hinch, D. K. (2015). Time-dependent deacclimation after cold acclimation in *Arabidopsis thaliana* accessions. *Sci. Rep.* 5, 12199. doi: 10.1038/srep12199
- Conflict of Interest:** The authors declare that the research was conducted in the absence of any commercial or financial relationships that could be construed as a potential conflict of interest.
- Copyright © 2019 Keller, Matsubara, Rascher, Pieruschka, Steier, Kraska and Muller. This is an open-access article distributed under the terms of the Creative Commons Attribution License (CC BY). The use, distribution or reproduction in other forums is permitted, provided the original author(s) and the copyright owner(s) are credited and that the original publication in this journal is cited, in accordance with accepted academic practice. No use, distribution or reproduction is permitted which does not comply with these terms.